

A conditional probability analysis of cystic fibrosis transmembrane conductance regulator gating indicates that ATP has multiple effects during the gating cycle

Daniel J. Hennager, Mutsuhiro Ikuma, Toshinori Hoshi, and Michael J. Welsh*

Howard Hughes Medical Institute, Departments of Internal Medicine and Physiology and Biophysics, University of Iowa College of Medicine, Iowa City, IA 52242

Contributed by Michael J. Welsh, December 29, 2000

ATP-binding cassette (ABC) transporters bind and hydrolyze ATP. In the cystic fibrosis transmembrane conductance regulator Cl^- channel, this interaction with ATP generates a gating cycle between a closed (C) and two open (O1 and O2) conformations. To understand better how ATP controls channel activity, we examined gating transitions from the C to the O1 and O2 states and from these open states to the C conformation. We made three main observations. First, we found that the channel can open into either the O1 or O2 state, that the frequency of transitions to both states was increased by ATP concentration, and that ATP increased the relative proportion of openings into O1 vs. O2. These results indicate that ATP can interact with the closed state to open the channel in at least two ways, which may involve binding to nucleotide-binding domains (NBDs) NBD1 and NBD2. Second, ATP prolonged the burst duration and altered the way in which the channel closed. These data suggest that ATP also interacts with the open channel. Third, the channel showed runs of specific types of open-closed transitions. This finding suggests a mechanism with more than one cycle of gating transitions. These data suggest models to explain how ATP influences conformational transitions in cystic fibrosis transmembrane conductance regulator and perhaps other ABC transporters.

Cystic fibrosis transmembrane conductance regulator (CFTR) is an epithelial Cl^- channel in the ATP-binding cassette (ABC) transporter family. CFTR activity is regulated by three intracellular domains, a regulatory (R) domain and two nucleotide-binding domains (NBD) (NBD1 and NBD2) (for review, see refs. 1 and 2). After phosphorylation of the R domain by cAMP-dependent protein kinase, the NBDs bind and hydrolyze ATP to open and close the channel. Earlier studies have revealed much about how ATP interacts with the two NBDs to control gating. For example, both NBDs contribute to ATP-dependent gating, and their interactions with ATP both open and close the channel (3–12).

Single-channel recordings of CFTR typically show bursts of openings with interspersed brief closures, separated by long closures (1, 2). This observation suggests that CFTR contains at least three kinetically distinguishable conformations: one open state, one short flickery closed state, and a long-lived closed state. An additional gating conformation was revealed when Gunderson and Kopito (6) identified two open states that appeared to have two different unitary amplitudes: O1 and O2. A subsequent study showed that these two open states represented two different sensitivities of the channel to block by the buffer 3-(*N*-morpholino)propanesulfonic acid (Mops) (13). In the O1 state, Mops blocked the open channel, creating a flickery pattern of block, whereas the O2 state represented an open channel conformation in which Mops block was minimal. Both studies suggested that the O1, O2, and C states were connected in asymmetric gating cycles and that transitions between the

three states violated microscopic reversibility consistent with energy input from ATP binding and hydrolysis.

The presence of two discernable open states provides a characteristic signature that allows further analysis of CFTR gating mechanisms. To understand better the gating mechanisms of CFTR, we analyzed the durations of open states that occurred adjacent to the long closed state to determine whether CFTR openings and closings occurred via the O1 or O2 state.

Materials and Methods

CFTR Expression. Wild-type CFTR was expressed in HeLa cells by using the vaccinia virus/T7 bacteriophage hybrid expression system, as previously described (3). Cells were studied 4–24 h after transfection.

Patch-Clamp Methods. The methods for excised inside-out patch-clamp were as described previously (5). Experiments were performed at room temperature. Holding voltage was -100 mV referenced to the external surface of the patch. An Axopatch 1-D amplifier (Axon Instruments, Foster City, CA) was used for voltage-clamping and current amplification. The PCLAMP 7.0.0.86 software package (Axon) was used for data acquisition and half-height threshold analysis. Records were filtered at 1 kHz by using a variable eight-pole Bessel filter (Frequency Devices, Haverhill, MA) and digitized at 100 kHz. CFTR was activated by excising into a bath solution containing 1 mM ATP (Mg^{2+} salt; Sigma) and 75 nM of the catalytic subunit of cAMP-dependent protein kinase (Promega). The pipette (extracellular) solution contained (in mM): 140 *N*-methyl-D-glucamine, 140 aspartic acid, 5 CaCl_2 , 10 *N*-Tris[hydroxymethyl]methyl-2-aminoethanesulfonic acid, pH 7.3, with HCl (Cl^- concentration, 10 mM). The bath (intracellular) solution contained (in mM): 140 *N*-methyl-D-glucamine, 135.5 HCl, 3 CaCl_2 , 3 MgCl_2 , 20 Mops, 1 CsEGTA, pH 7.3, with HCl (Cl^- concentration, 146 mM). To achieve a zero concentration of ATP, we washed the nucleotide out thoroughly (30 ml, chamber volume 0.5 ml) and added hexokinase (12 units/ml) and glucose (10 mM) to hydrolyze any ATP that might remain in the bath after a solution change (14). Under these conditions, we did not detect ATP by using a luciferase assay (not shown) (15).

Data Analysis. Events lists generated by half-height threshold analysis from each experiment were used to construct closed

Abbreviations: CFTR, cystic fibrosis transmembrane conductance regulator; ABC, ATP-binding cassette; NBD, nucleotide-binding domain; Mops, 3-(*N*-morpholino)propanesulfonic acid.

*To whom reprint requests should be addressed at: Howard Hughes Medical Institute, University of Iowa College of Medicine, 500 EMRB, Iowa City, IA 52242. E-mail: mjwelsh@blue.weeg.uiowa.edu.

The publication costs of this article were defrayed in part by page charge payment. This article must therefore be hereby marked "advertisement" in accordance with 18 U.S.C. §1734 solely to indicate this fact.

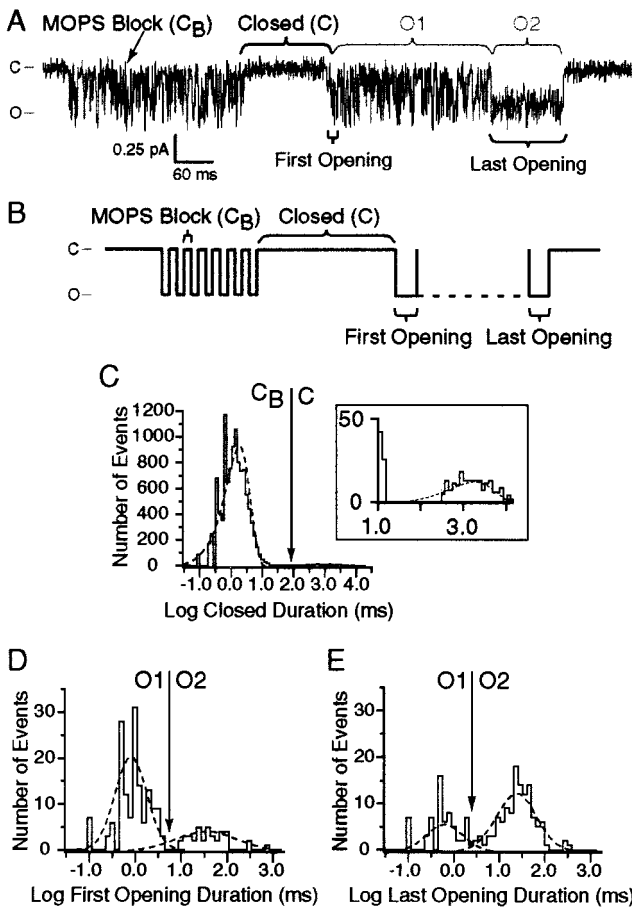


Fig. 1. Gating of CFTR Cl^- channels. (A and B) Real (A) and schematic (B) current traces are shown to depict the four kinetic states of CFTR; closed (C), blocked (C_B), an open state susceptible to Mops block (O1), and an open state less susceptible to Mops block (O2). Openings adjacent to the channel closed state (C), the first and last openings, were identified as the O1 or O2 state on the basis of their duration. (C) Closed duration histograms. Closures were identified as C or C_B by using a delimiter of 79 ms (arrow). Dashed lines indicate time constants as determined by a least-square fit to the sum of two exponentials. *Inset* shows long-duration event with expanded axes. (D) Duration histograms of first openings. Data were fit by two exponentials (dashed lines). The short openings ($\tau = 0.86$ ms) represent O1, and the longer openings ($\tau = 34.88$ ms) represent O2. The nadir (5.75 ms; arrow) delineated the two distributions. (E) Duration histograms of last openings. Two exponentials (dashed lines) identify O1 openings ($\tau = 0.86$ ms) and O2 openings ($\tau = 33.30$ ms). Arrow indicates the nadir (2.04 ms). Data are representative examples from experiment no. 1006.

duration histograms (10 bins/decade) by using EXCEL software (Microsoft). Curve fits, generated with PSTAT (Axon), were used to determine time constants of kinetic states. Closed-duration histograms were used to separate short closures within bursts that are caused by Mops block (C_B) from long closures between bursts (C) (16). Bursts were defined as channel activity that occurred between two consecutive C states. Duration histograms for first and last openings were generated from the events that preceded and followed each C state. Each histogram was best fit by a sum of two exponentials, indicating two distributions of openings. Curve fits determined the nadir between the two distributions. These nadirs were subsequently used to distinguish whether CFTR was in the O1 state (characterized by short openings because of Mops block) or the O2 state (characterized by longer openings). A burst was then classified on the basis of the state (O1 or O2) into which it first opened and the last open state (O1 or O2) before closing.

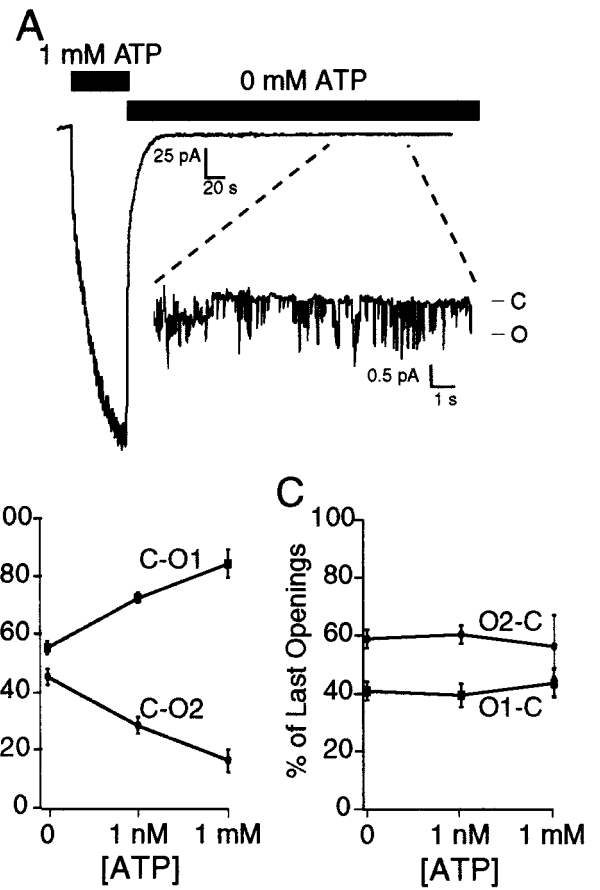


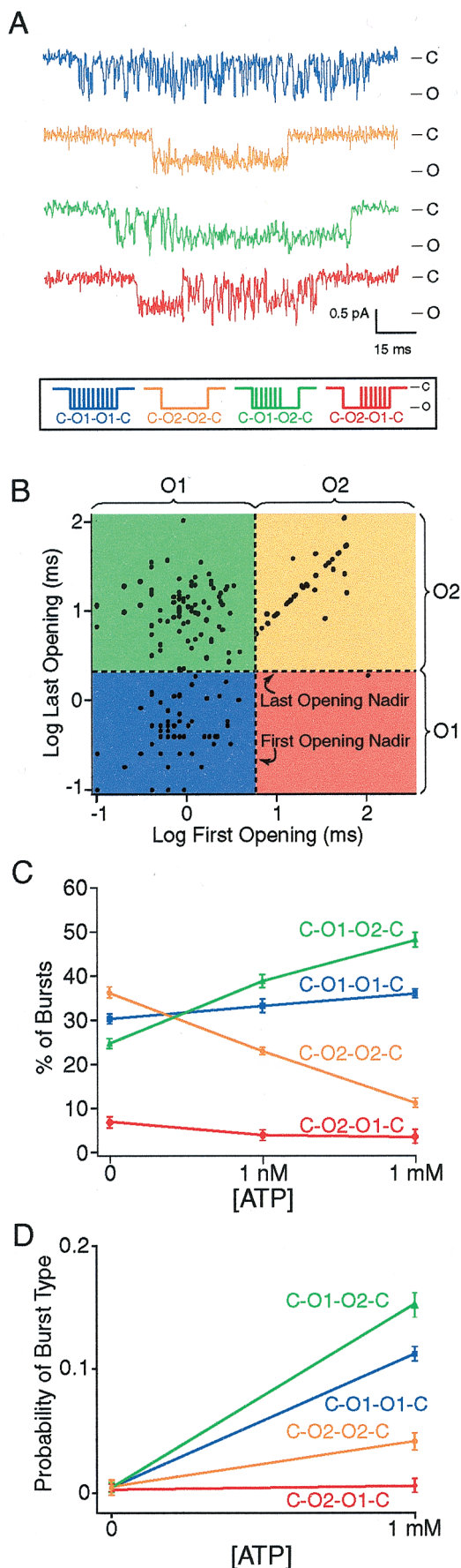
Fig. 2. Effect of ATP on CFTR opening and closing. (A) Membrane patch containing multiple CFTR channels with cytosolic surface exposed to ATP (1 mM) and cAMP-dependent protein kinase (75 nM) or zero ATP (12 units/ml hexokinase and 10 mM glucose) during times indicated by bars. *Inset* shows that channel opened rarely in zero ATP. (B) Percentage of first openings that were transitions to O1 or O2. (C) Percentage of last openings that were O1-C and O2-C transitions. Data are means \pm SEM for $n = 5, 5,$ and 7 channels at $0, 1$ nM, and 1 mM ATP, respectively.

Data are shown as mean \pm SEM. A Student's *t* test was used to test statistical significance. A Kolmogorov–Smirnov analysis was used to compare distributions in event duration histograms (17).

Results

Identification of Transitions Between the Closed and Open States. Fig. 1 shows an actual (A) and a schematic (B) trace of current from a single CFTR channel. These traces show the four kinetically distinguishable states of CFTR (on this timescale): closed (C), blocked (C_B), O1, and O2. The C state is the closed state between bursts of activity. The C_B state occurs when Mops blocks an open channel, giving rise to short closings; in the absence of Mops or a related buffer, this state is not apparent (13). In the O1 state, the channel is open, but the openings appear flickery because of a fast Mops block. In the O2 state, Mops does not cause a flickery block, and openings are relatively free of short closures. In this study, our analyses were based on transitions adjacent to the C state. Therefore, we first distinguished the C from the C_B state (Fig. 1A).

Fig. 1C shows the closed-duration histogram from a representative single-channel experiment. Two distinct populations are apparent: a short-duration closed state with a mean duration of ≈ 2.0 ms and a long-duration closed state of ≈ 2 sec. We used



a value of 79 ms (arrow) as the criterion to distinguish C from C_B , because this value fell within the nadir of populations of closed times for 16 of 17 experiments. Values for τ and the area from closed-duration histograms from all experiments are shown in Table 1, which is published as supplemental data on the PNAS web site, www.pnas.org.

With the ability to discriminate C and C_B states, we asked whether the channel opened from the C state into the O1 or O2 state (Fig. 1A and B). To do this, we measured the duration of the first opening after a C state. Duration histograms distinguished two populations (Fig. 1D), one with a short mean duration ($\tau = 0.86$ ms) and one with a longer duration ($\tau = 35$ ms). The supplementary material provides data for individual experiments. We used the nadir between the two distributions (5.75 ms for the example in Fig. 1D; arrow) to distinguish an opening as either O1 or O2 and thereby define first openings as either C-O1 or C-O2 transitions. With 1 mM ATP, the channel opened into the O1 state $83.1 \pm 1.1\%$ of the time, whereas only $16.9 \pm 1.1\%$ of the openings were C-O2 ($n = 7$, $P < 0.001$).

Using a similar method, we determined whether CFTR entered the C state from the O1 or the O2 state (O1-C vs. O2-C). Fig. 1E shows a histogram of the duration of the last opening before the transition to the C state; two populations are apparent: one short ($\tau = 0.86$ ms) and one longer ($\tau = 33.30$ ms). A nadir value of 2.04 ms separated the two distributions (arrow, Fig. 1E). Supplementary material provides primary raw data for all of the experiments (www.pnas.org). We used this nadir to identify O1-C and O2-C transitions. Bursts ended by closing from the O1 state $41.3 \pm 1.3\%$ of the time and closing from the O2 state $58.7 \pm 1.3\%$ of the time ($P < 0.001$).

Effect of ATP Concentration on Transitions into and out of the Open State.

Increasing the ATP concentration increases the rate of opening (3, 10, 11, 18–21). Therefore, we asked whether ATP influenced opening into O1 or O2. To enhance our ability to detect changes, we varied ATP in a wide concentration range. We used multichannel patches to examine the effect of zero ATP (see *Materials and Methods*) (Fig. 2A). When we reduced the ATP concentration from 1 to 0 mM (see *Materials and Methods*), mean current amplitude decreased $99.3 \pm 0.2\%$ ($n = 4$). Assuming a constant number of channels and constant single-channel amplitude, removing ATP reduced P_O to 0.7% of the value at 1 mM ATP. Thus, we observed some channel openings in the absence of ATP, albeit at a very low frequency. These open events were because of CFTR on the basis of their unitary amplitude, Mops block, and presence only in cells expressing CFTR (not shown). In the remainder of the experiments, we used multichannel patches when examining the effect of 0 or 1 nM ATP and single-channel patches when examining the effect of 1 mM ATP.

In the absence of ATP, there was only a small difference between the proportion of C-O1 and C-O2 openings (Fig. 2B). Thus neither transition was markedly favored. However, as the concentration of ATP increased, the relative proportion of C-O1

Fig. 3. CFTR exhibits four burst types that are differentially affected by ATP. (A) Examples of the four burst types, indicated by color. (B) Plot of logarithm (log) duration of first openings vs. log duration of last openings (experiment no. 1006). O1 and O2 states were differentiated by using nadirs from duration histograms (dashed lines). Much of the data in the C-O2-O2-C box (orange) fall on a line because in these burst types, the first and last opening were often the same. (C) Relative frequency of each burst type at indicated ATP concentration. (D) Probability of each burst type at 0 and 1 mM ATP. Probability of a burst type was calculated as relative burst frequency (C) multiplied by P_O . At 1 mM ATP, P_O was 0.3 and at 0 mM ATP, P_O was estimated to be 0.002. All burst types increased ($P < 0.05$) except C-O2-O1-C transitions. Data are mean \pm SEM. $n = 5$ at 0 ATP and 7 at 1 mM ATP.

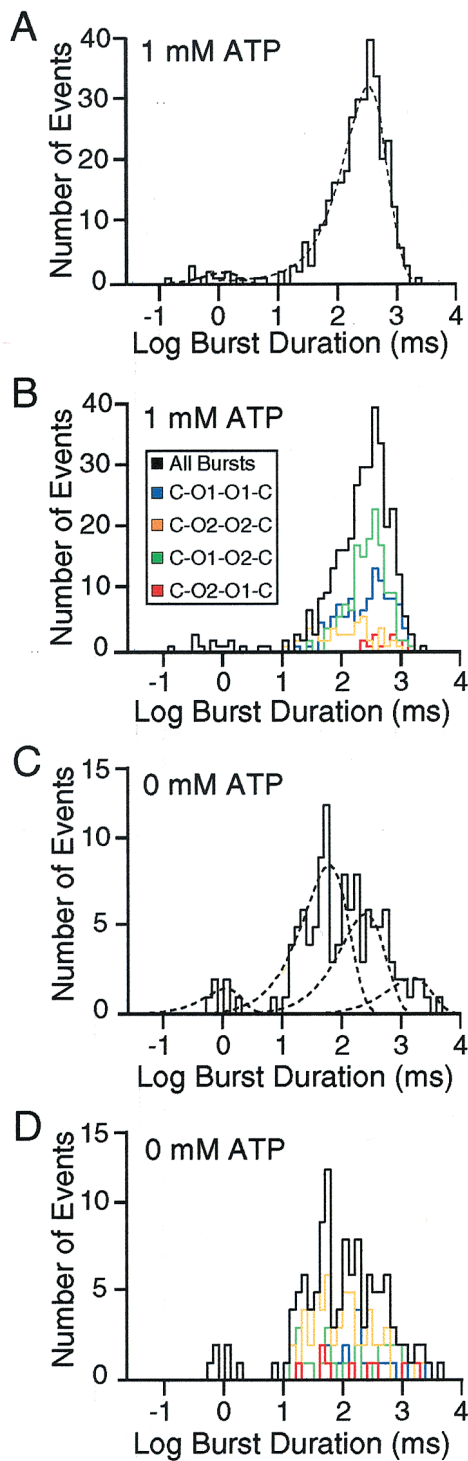


Fig. 4. Effect of ATP on burst duration. Data are examples from experiment no. 1003 at 1 mM ATP (A and B) and no. 82707 at zero ATP (C and D). (A and C) Duration histograms for all bursts. Dashed lines show exponentials required to fit the data as evaluated by the logarithm likelihood method. (B and D) Duration histograms for each of the different burst types, as indicated.

transitions increased, whereas the proportion of C-O2 transitions fell (Fig. 2B). On the basis of the effect of ATP on P_{O_0} and the small effect on burst duration (see below), we estimated that 1 mM ATP increased the average opening rate 112-fold, as compared with zero ATP. This very large increase in ATP-induced opening frequency suggests that the absolute frequency

of both C-O1 and C-O2 transitions increased even though the relative frequency of C-O2 transitions fell.

We also examined the transition from the two open states to the closed state. In contrast to the first opening, ATP did not influence the average frequency of closing through the O1 and O2 states (Fig. 2C).

Effect of ATP Concentration on Types of Bursts. On the basis of how the channel enters and exits each burst event, four burst types are possible: C-O1-O1-C, C-O2-O2-C, C-O1-O2-C, and C-O2-O1-C. Consistent with earlier reports (6, 13), we observed all four burst types in our recordings (Fig. 3A). Fig. 3B shows data from one experiment where the duration of the first opening is plotted against the duration of the last opening. Dashed black lines represent nadirs between O1 and O2 states from first and last opening histograms. This graph shows that bursts began and ended in both the O1 and O2 states, that all four burst types occurred, and that burst types occur with markedly different frequency (for example, in Fig. 3B, only one C-O2-O1-C event occurred).

The relative frequencies of some burst types depended on the ATP concentration (Fig. 3C). ATP increased the relative frequency of C-O1-O2-C events and reduced that of C-O2-O2-C events ($P < 0.001$) (Fig. 3C). ATP had minimal effects on the relative frequencies of C-O1-O1-C or C-O2-O1-C burst types. These data suggest that, in addition to affecting closed to open transitions, ATP also interacts with the channel when it is in a burst to influence closing via the O1 or O2 states. To illustrate this point, consider those channels that enter a burst via a C-O1 transition. In zero ATP, there is a similar likelihood that the channel will exit via O1 or O2 (C-O1-O1-C has a similar frequency as C-O1-O2-C). However, as ATP concentration increased, the relative frequency of C-O1-O2-C became greater than C-O1-O1-C ($P < 0.01$) (Fig. 3C). This result suggests that ATP has some action after the initial C-O1 transition; if ATP affected only C-O1, then ATP should similarly affect the frequency of C-O1-O1-C and C-O1-O2-C burst types. An alternative interpretation is that there is more than one O1 state that we cannot distinguish. ATP also had different effects on C-O2-O2-C vs. C-O2-O1-C transitions.

Although ATP altered the relative proportion of some burst types in opposite directions, because of the large increase in activity induced by ATP addition, it increased the absolute frequency of all burst types except C-O2-O1-C; Fig. 3D shows an estimate of the probability of the different burst types at 0 and 1 mM ATP.

Burst Duration Is Influenced by ATP Concentration. Because our data suggested that ATP interacts with the open state, we hypothesized that ATP might alter the burst duration. One study did not detect a significant effect on burst duration of varying ATP from 0.1 to 3 mM (22). However, two other studies suggested that increasing ATP concentration increased burst duration (11, 19). This difference may be related in part to the experimental temperature, 37°C (22), vs. room temperature (11, 19). To further test the effect of ATP, we compared burst duration at the extremes of 0 and 1 mM ATP. Average burst duration increased from 184 ± 11 ms to 286 ± 28 ms when ATP concentration increased ($P < 0.05$) (Fig. 4). At 1 mM ATP, burst durations were well fit to a sum of two exponentials, but at zero ATP, three or four exponential components were required (Fig. 4A and C). The requirement for three to four exponentials to fit burst durations at zero ATP suggests the presence of multiple paths by which the channel can close. Thus, when the channel does open, albeit rarely at zero ATP, it can follow multiple different pathways to close. The presence of ATP may constrain the channel to more ordered behavior, thereby reducing the number of exponentials required to fit the data.

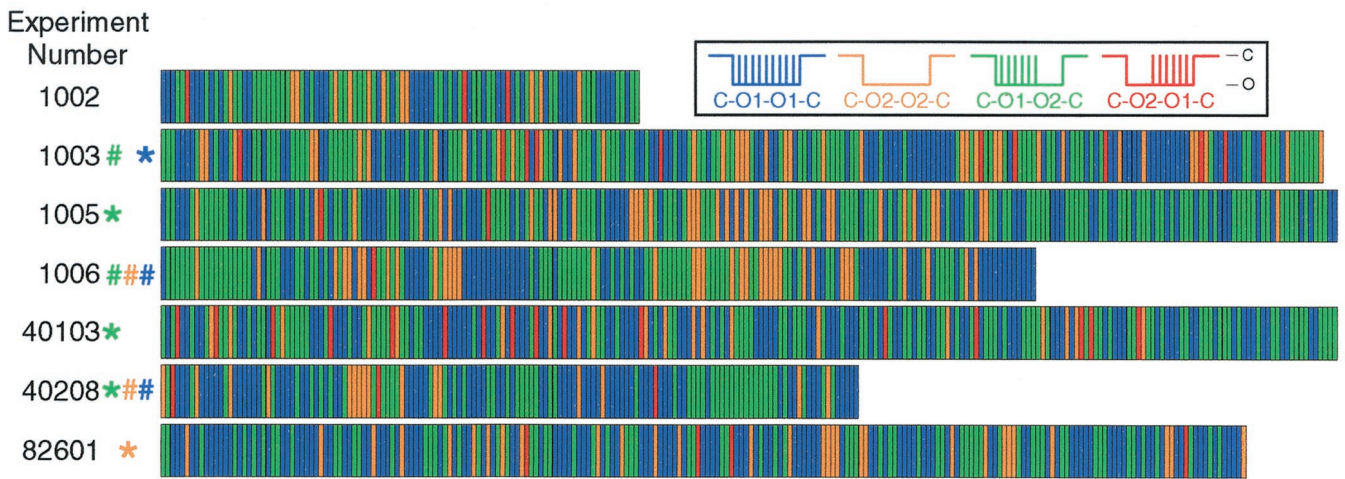


Fig. 5. Sequential occurrence of burst types in patches containing a single channel. Colored bars represent burst type. Clustering of the various burst types was tested by using a runs analysis, and statistical significance is shown to left of bar, as indicated (color corresponds to burst type that clustered). *, $P < 0.05$; #, $P < 0.01$.

Burst Types Sometimes Occur in Runs. We examined the sequence of burst types, because the presence or absence of order between adjacent bursts has important implications for the mechanism of gating. Fig. 5 shows a schematic representation of the burst sequence obtained from seven separate single channel experiments. Individual burst types are represented by different colors.

To determine whether runs of burst types occurred more or less often than predicted by chance alone, we used a runs analysis, which compares the probability of an individual event to the probability that the event occurs in clusters (16). In five of seven experiments, C-O1-O2-C burst types clustered ($P < 0.05$) (Fig. 5). Moreover, in three of seven experiments, C-O1-O1-C and C-O2-O2-C burst types occurred in runs ($P < 0.05$). In contrast, we did not observe clustering of C-O2-O1-C burst types. These data indicate a relationship exists between bursts.

Clustering of burst types suggested bursts within a run might be separated by unique C states. Therefore, we examined whether C states could be kinetically distinguished by categorizing C states according to whether they occurred between the same burst type (e.g., the closed states that occurred between sequential C-O1-O1-C bursts were put into one histogram, the closed states that occurred between sequential C-O1-O2-C bursts were put into another histogram, etc.). In six of seven experiments, the C state between sequential C-O1-O1-C bursts was significantly shorter than the average; Fig. 6 shows an example. We found no significant difference between C states that occurred within runs of other burst types. These data suggest a unique closed state within C-O1-O1-C runs and, although we could not distinguish multiple closed states within runs of other burst types by these criteria, the data do not preclude their existence.

Discussion

Earlier studies of the effects of ATP concentration, nucleoside analogs, site-directed mutations, and chemical modifications have established the central role of the NBDs and ATP in controlling CFTR channel gating (3–12). However, the molecular mechanisms of gating, including the function of the individual NBDs and their interactions remain uncertain. Consequently, investigators have proposed several models to describe CFTR gating (1, 2, 4–6, 10–12, 20). Most recent models account for the following features of ATP-dependent gating: (i) ATP binding alone is able to open the channel (9, 12, 20, 23, 24); (ii) ATP hydrolysis initiates conformational changes that ultimately lead to channel closure (the channel can also close with ATP

dissociation) (1, 2, 6, 10–12); (iii) ATP binding and hydrolysis by either NBD enables channel gating (4, 12); (iv) the two NBDs interact functionally (9, 11, 12, 19, 25).

By analyzing gating using two distinguishable open conformations, this study allows significant modifications and extensions of earlier models and raises interesting questions about the gating mechanisms. However, our study was also limited in that we studied only transitions adjacent to the C state. Thus, O1 and O2 transitions between the first and last openings were not examined, which prevents us from assessing how ATP interacts with the open state.

ATP-Dependent Opening. Our findings suggest a minimal model for the opening step (Fig. 7). The channel can open into either the O1 or the O2 state. In the absence of ATP, openings were rare, but when they did occur, C-O1 and C-O2 transitions occurred with approximately similar frequency. As ATP concentration increased, both transitions became more common, even though C-O1 transitions were favored over C-O2. This

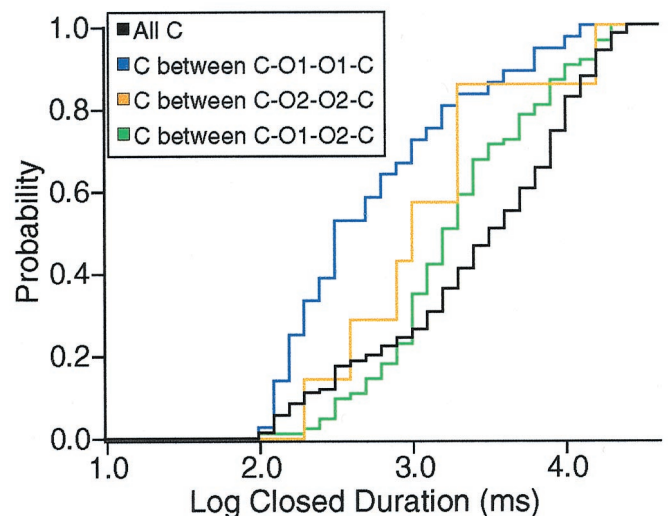


Fig. 6. Cumulative distributions of the closed durations between like burst types. Data are from experiment no. 40208. C durations between C-O1-O1-C bursts were different from the mean ($P < 0.001$).

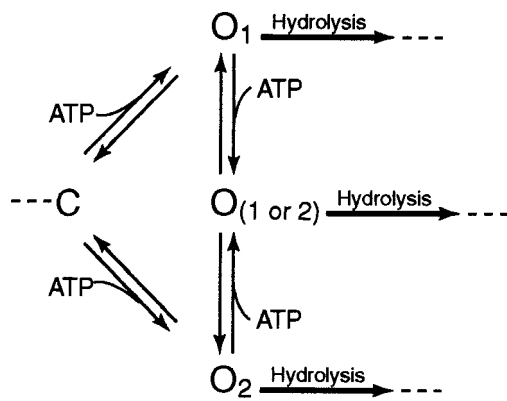


Fig. 7. Minimal model of ATP effect on gating. See text for details. Dashed lines indicate additional states that we do not define. (Left) Channel cycles through these and probably other states to return to the C state.

result suggests that both C-O1 and C-O2 are ATP-dependent steps, although in a strict sense, C-O1 and C-O2 need not represent the actual ATP-binding events. The preponderance of C-O1 over C-O2 in the presence of ATP could be explained by rate constants with dissimilar ATP-binding kinetics. When the channel opens, it may move between O1 and O2 without terminating the burst, suggesting direct connections between these two open states (Fig. 7).

It is tempting to speculate that C-O1 and C-O2 transitions result from ATP binding to separate NBDs. Perhaps ATP binding to NBD1 leads to O1 and ATP binding to NBD2 leads to O2. Consistent with this hypothesis, mutations that likely decrease ATP binding at NBD2 increase the relative frequency of C-O1 (6). Whether equivalent mutations at NBD1 increase C-O2 transitions is not known. A result not readily explained by this model is our earlier finding that blocking ATP binding by covalent modification of either NBD1 or NBD2 markedly reduced opening rate (7). We speculate that interactions between the two NBDs account for this result.

ATP-Dependent Closing. Two observations suggest that ATP interacts with a channel in a burst to influence closing. First, raising ATP concentration from 0 to 1 mM extended the burst duration, although the 1.5-fold effect was relatively modest. This result is consistent with earlier observations (11, 19). We also found that ATP prolonged the duration of all burst types and reduced the number of exponential components required to fit burst durations, which suggests that ATP influences the number of states

the channel traverses before closure. The significance of this observation is unknown. Second, ATP influenced the mechanism of closing. For example, after channels opened into the O1 state, ATP increased the likelihood that they closed via O2, i.e., the proportion of C-O1-O2-C increased more than C-O1-O1-C (Fig. 3C). Likewise, for channels that opened into O2, ATP biased the state from which the channel closed.

To explain these data, we suggest that a single ATP may open CFTR and binding a second ATP may carry it to a new state and/or stabilize the open channel (Fig. 7). This model has some similarity to that of Zeltwanger *et al.* (11), with the exception that their model proposes that ATP hydrolysis must occur before opening. When ATP binds, there are three alternatives: ATP can dissociate to close the channel, the channel can hydrolyze ATP to close, or ATP can bind to the other NBD to extend the open state. Such a model could account for the effect of ATP on burst duration, the multiple-exponentials required to fit burst durations, and the influence of ATP on the way in which the channel closes.

Runs of Burst Types. Interestingly, we found that the sequence of burst types was not random. Instead, the channel sometimes repeatedly went through the same burst type. This phenomenon cannot be explained by a linear gating model or a model containing a single gating cycle. However, the partial model of the gating cycle shown in Fig. 7 could generate such activity. For example, repeated cycles of ATP binding (and hydrolysis) at one or the other NBD could generate runs of activity. Moreover, ATP-dependent allosteric interactions between the NBDs might facilitate runs of different burst types.

The potential complexity of CFTR gating is emphasized by the large number of conformations that the protein might possibly adopt, e.g., nucleotide-free, ATP-bound, ADP- and Pi-bound, and transition states. Moreover there are two NBDs that interact with ATP and with each other. Deciphering which of these potential conformations correspond to the various open and closed states is important to understanding how CFTR works and how other ABC transporters function. Our data investigating how ATP affects transitions into and out of the open state provide insight into the gating process and suggest models for the molecular mechanisms involved.

We thank Pary Weber, Tamara Nesselhauf, and Theresa Mayhew for excellent assistance, and our laboratory colleagues for helpful discussions. We also thank Nelson Lu and the Statistical Consulting Center for their assistance. This work was supported by the National Institutes of Health (HL-29851 to M.J.W. and GM57654/HL61645 to T.H.) and the Howard Hughes Medical Institute (HHMI). M.J.W. is an Investigator of the HHMI.

- Sheppard, D. N. & Welsh, M. J. (1999) *Physiol. Rev.* **79**, S23–S45.
- Gadsby, D. C. & Nairn, A. C. (1999) *Physiol. Rev.* **79**, S77–S107.
- Anderson, M. P., Berger, H. A., Rich, D. P., Gregory, R. J., Smith, A. E. & Welsh, M. J. (1991) *Cell* **67**, 775–784.
- Hwang, T. C., Nagel, G., Nairn, A. C. & Gadsby, D. C. (1994) *Proc. Natl. Acad. Sci. USA* **91**, 4698–4702.
- Carson, M. R., Travis, S. M. & Welsh, M. J. (1995) *J. Biol. Chem.* **270**, 1711–1717.
- Gunderson, K. L. & Kopito, R. R. (1995) *Cell* **82**, 231–239.
- Cotten, J. F. & Welsh, M. J. (1998) *J. Biol. Chem.* **273**, 31873–31879.
- Mathews, C. J., Tabcharani, J. A. & Hanrahan, J. W. (1998) *J. Membr. Biol.* **163**, 55–66.
- Ramjeesingh, M., Li, C., Garami, E., Huan, L. J., Galley, K., Wang, Y. & Bear, C. E. (1999) *Biochemistry* **38**, 1463–1468.
- Weinreich, F., Riordan, J. R. & Nagel, G. (1999) *J. Gen. Physiol.* **114**, 55–70.
- Zeltwanger, S., Wang, F., Wang, G. T., Gillis, K. D. & Hwang, T. C. (1999) *J. Gen. Physiol.* **113**, 541–554.
- Ikuma, M. & Welsh, M. J. (2000) *Proc. Natl. Acad. Sci. USA* **97**, 8675–8680. (First Published July 4, 2000; 10.1073/pnas.140220597)
- Ishihara, H. & Welsh, M. J. (1997) *Am. J. Physiol.* **273**, C1278–C1289.
- Carson, M. R. & Welsh, M. J. (1993) *Am. J. Physiol.* **265**, L27–L32.
- Jiang, Q., Mak, D., Devidas, S., Schwiebert, E. M., Bragin, A., Zhang, Y., Skach, W. R., Guggino, W. B., Foskett, J. K. & Engelhardt, J. F. (1998) *J. Cell. Biol.* **143**, 645–657.
- Sakmann, B. & Neher, E. (1983) *Single-Channel Recording* (Plenum, New York).
- Conover, W. J. (1980) *Nonparametric Statistics* (Wiley, New York).
- Winter, M. C., Sheppard, D. N., Carson, M. R. & Welsh, M. J. (1994) *Biophys. J.* **66**, 1398–1403.
- Li, C., Ramjeesingh, M., Wang, W., Garami, E., Hewryk, M., Lee, D., Rommens, J. M., Galley, K. & Bear, C. E. (1996) *J. Biol. Chem.* **271**, 28463–28468.
- Schultz, B. D., Bridges, R. J. & Frizzell, R. A. (1996) *J. Membr. Biol.* **151**, 63–75.
- Mathews, C. J., Tabcharani, J. A., Chang, X. B., Jensen, T. J., Riordan, J. R. & Hanrahan, J. W. (1998) *J. Physiol.* **508**, 365–377.
- Winter, M. C. & Welsh, M. J. (1997) *Nature (London)* **389**, 294–296.
- Reddy, M. M. & Quinton, P. M. (1996) *Am. J. Physiol.* **271**, C35–C42.
- Aleksandrov, A. A. & Riordan, J. R. (1998) *FEBS Lett.* **431**, 97–101.
- Anderson, M. P. & Welsh, M. J. (1992) *Science* **257**, 1701–1704.